Hindawi Publishing Corporation
International Journal of Polymer Science
Volume 2015, Article ID 758474, 7 pages
http://dx.doi.org/10.1155/2015/758474

*Research Article*

# The Mechanical Aspects of Formation and Application of PDMS Bilayers Rolled into a Cylindrical Structure

**Dongwon Kang, Hyeonji Yu, and Jungwook Kim**

*Department of Chemical and Biomolecular Engineering, Sogang University, 1 Sinsu-dong, Mapo-gu, Seoul 121-742, Republic of Korea*

Correspondence should be addressed to Jungwook Kim; jungwkim@sogang.ac.kr

Received 18 March 2015; Revised 29 April 2015; Accepted 3 May 2015

Academic Editor: Ming Tian



A polydimethylsiloxane (PDMS) film with its surface being oxidized by a plasma treatment or a UV-ozone (UVO) treatment, that is, a bilayer made of PDMS and its oxidized surface layer, is known to roll into a cylindrical structure upon exposure to the chloroform vapor due to the mismatch in the swelling ratio between PDMS and the oxidized layer by the chloroform vapor. Here we analyzed the formation of the rolled bilayer with the mechanical aspects: how the mismatch in the swelling ratio of the bilayer induces rolling of the bilayer, why any form of trigger that breaks the symmetry in the in-plane stress level is needed to roll the bilayer uniaxially, why the rolled bilayer does not unroll in the dry state when there is no more mismatch in the swelling ratio, and how the measured curvature of rolled bilayer matches well with the prediction by the theory. Moreover, for the use of the rolled bilayer as the channel of the microfluidic device, we examined whether the rolled bilayer deforms or unrolls by the flow of the aqueous solution that exerts the circumferential stress on the rolled bilayer.

## 1. Introduction

When the thin film experiences the in-plane stress that is inhomogeneous along the thickness direction, the film rolls into a cylindrical structure provided that the film is both thin and long enough. One simple method to obtain such inhomogeneity of the in-plane stress along the film thickness is to have two films with dissimilar in-plane stresses to attach to each other, that is, form a bilayer. Bilayers made of polymer films with uneven in-plane stresses can be fabricated by attaching the stretched (or compressed) film to the stress-free film. Alternatively, they can be obtained by swelling the bilayer made of two stress-free films by the solvent that swells each film in a different swelling ratio [1–6]. The latter method has been used frequently as the swelling ratio of each polymeric film, defined as the volumetric ratio of the film swollen in the solvent to that in the dry state, can be easily controlled by variables such as solvent quality, crosslinking density, or density of polymeric network [7]. If the bilayer is sufficiently thin, the primary mode of releasing the elastic strain energy generated by unevenness of the in-plane stress level is to bend out-of-plane and eventually roll if the bilayer is long enough. If one layer is much thicker than the other, the thicker layer resists out-of-plane bending, and the bilayer undergoes different types of deformations such as wrinkling, folding, or irreversible cracking [1–3, 5, 6, 8–12]. The rolled bilayer has been made of different materials such as polymers [4, 13–16], metals and semiconductors [17–20], or composites [21] and used in various applications including X-ray waveguide [17], microfluidic system [4], optical resonators [18], and microcapsules capable of controlled capture and release of cells [15].

It has been theoretically predicted that the curvature of rolled polymeric bilayer can be determined by swelling ratio (strain), thickness, and elastic modulus of each layer at its stress-free state [22]. With this respect, the bilayer made of PDMS is of particular interest because elastic modulus and swelling ratio of PDMS can be systematically controlled by varying the base to curing agent ratio and the solvent quality, which had already been studied in a number of literatures [4, 12, 23, 24]. Moreover, when the surface of PDMS is oxidized by a plasma treatment or a UVO treatment, it is well known that glass-like silica layer forms on the surface of PDMS with several tens of nanometers in thickness [24].

Such oxidized surface layer swells in a different ratio by most solvents when compared to the untreated (bulk) layer of PDMS. Therefore, the PDMS bilayer experiences in-plane elastic stress and rolls if the bilayer is thin enough. While a few studies have fabricated the rolled PDMS bilayer [4], the underlying mechanism of the fabrication has not been fully addressed with the mechanical aspects. In the current study, we provided mechanical analysis on the formation of the rolled PDMS bilayer with a number of mechanical aspects: the swelling mismatch, the need for breaking the symmetry of the in-plane stress level for the uniaxial rolling, the order of magnitude analysis for the adhesion energy and the elastic strain energy for maintaining the cylindrical shape, and the comparison between the measured curvatures of rolled bilayers and the theoretical values predicted by Timoshenko's model. Moreover, relative strength between the hoop stress and the frictional force per unit area has been compared for utilizing the rolled PDMS bilayer as the microfluidic channel.

## 2. Materials and Methods

*2.1. Materials.* 4-Vinylpyridine (4VP), azobisisobutyronitrile (AIBN), and rhodamine B were purchased from Aldrich and used as received. PDMS (Sylgard 184) was purchased from Dow Corning. Tygon tubing (Tygon S-50-HL PVC tubing) was used for the perfusion test.

*2.2. Synthesis of Poly(4-vinylpyridine) (P4VP).* P4VP was synthesized by the free radical polymerization of 4VP. Briefly, 1 mL of 4VP and 5 mg of AIBN were dissolved in 5 mL of ethanol in a 25 mL round-bottom flask connected to a condenser. The solution was purged with nitrogen for 30 min and immersed in an oil bath maintained at 70°C for two hours. The product was precipitated in cold diethyl ether, filtered, and dried in the vacuum oven.

*2.3. Fabrication of Surface Oxidized PDMS Bilayer on P4VP Coated Glass Substrate.* A 0.1 wt% solution of P4VP in chloroform was spin-coated at 1500 rpm for 1 min on the glass substrate cleaned by the oxygen plasma treatment (CUTE-1MPR, Femto Science, 100 W) for 3 min. After evaporating residual solvent in the P4VP film, PDMS with a base to curing agent ratio of 10 : 1 was spin-coated on the P4VP coated substrate at 1000, 1500, 3000, or 4000 rpm to obtain PDMS films with varying thickness. The spin-coated PDMS films were cured at 120°C overnight. Fully cured PDMS films were oxidized by the oxygen plasma treatment (100 W for 30 min) to generate thin oxide layers on the surfaces of PDMS films. A thickness of PDMS films was measured using optical microscope (Zeiss AxioVert A1, 5x and 10x objectives) after detaching the films from the substrate.

*2.4. Formation of Rolled PDMS Bilayer.* The surface oxidized PDMS bilayer on the P4VP coated substrate (PDMS/P4VP substrate) was placed on the glass Petri dish inside the glass jar. A few drops of chloroform wetted the bottom of the jar but were not in direct contact with the PDMS/P4VP substrate. The jar was partially closed and placed on the hot plate maintained at 40°C to increase the vapor pressure of chloroform. The oxidized PDMS bilayer was found to gradually detach from the substrate and roll. After the completion of rolling, the rolled PDMS bilayer was dried in atmospheric air. A cross section of the rolled bilayer was imaged with optical microscope after cutting the rolled bilayer along the direction perpendicular to the cylindrical axis using a razor blade.

*2.5. Perfusion of Aqueous Solution through the Rolled PDMS Bilayer.* The rolled bilayer was used as the microfluidic channel by connecting it with Tygon tubing (inlet and outlet channels) via small pieces of PDMS on the glass substrate. An aqueous solution of rhodamine B (0.7 mmol in water) was manually injected into the microfluidic channel using a syringe at a volumetric flow rate of roughly 1 mL/min. A flow of the rhodamine B solution through the channel was sequentially imaged with a digital camera.

## 3. Results and Discussion

Cured PDMS is known to swell by chloroform to a large extent as a solubility parameter $\delta$ of PDMS (7.3 $\text{cal}^{1/2}\ \text{cm}^{-3/2}$) is close to that of chloroform (9.2 $\text{cal}^{1/2}\ \text{cm}^{-3/2}$). The linear swelling ratio of cured PDMS, defined as the ratio of the length of PDMS in the solvent to that of the dry PDMS, in a liquid chloroform is 1.39 [23]. P4VP is also highly soluble in chloroform. Therefore, when the PDMS/P4VP substrate was exposed to the chloroform vapor, a large amount of chloroform was absorbed in both P4VP layer and untreated PDMS layer, which significantly lowered the interfacial tension and therefore the adhesion energy between the two layers. As a result of lowered adhesion energy and swelling of untreated PDMS by chloroform vapor, we observed that the PDMS bilayer spontaneously detached from the glass substrate, initiating from the sides of the substrate that have higher surface-to-volume ratios than the interior. On the other hand, the silica-like oxidized PDMS swells negligibly by chloroform when compared to the untreated PDMS [23]. Therefore, a large difference in the in-plane stress is generated, a tension in the oxidized layer and a compression in the untreated layer, with the maximum in-plane stress occurring at the interface of two layers. If the thickness of the bilayer is sufficiently thin, the primary mode of releasing the in-plane stress is to bend out-of-plane. This is because the elastic deformation energy generated by bending out-of-plane scales with $t^3$ ($t$ is a bilayer thickness) whereas that by the in-plane stretching scales linearly with $t$. Therefore, the energy generated by the in-plane stretching due to the swelling mismatch of the PDMS bilayer can be released to a large extent by the out-of-plane bending of the bilayer, which costs much less energy at a sufficiently small $t$. Here, the criterion for a sufficiently small $t$ depends on other variables such as swelling ratio and elastic modulus of each layer.

Upon detachment from the glass substrate after exposure to the chloroform vapor, PDMS bilayers with $t$ varying from 12 $\mu$m to 67 $\mu$m were observed to roll into a cylindrical structure as illustrated in Figure 1. For thicker bilayers (33 $\mu$m

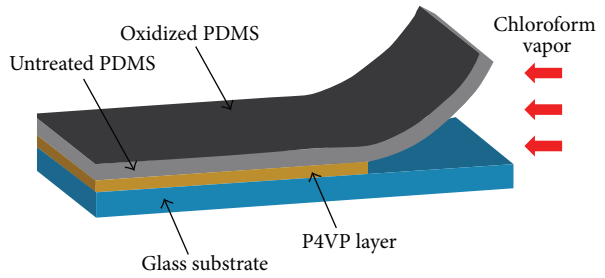


Figure 1: A schematic illustration of uniaxial rolling of the PDMS bilayer detached from the P4VP coated glass substrate upon exposure to the chloroform vapor.

and 67 $\mu$m), rolling was initiated with the help of the manual trigger; we used a tweezer to gently push the edge of the bilayer that is initially detached from one side of the substrate toward the opposite side of the substrate. We infer that such initial trigger is needed as it breaks the symmetry of the in-plane stress level present in the bilayer. As the bilayer experienced the equibiaxial stress, it started to roll from all four sides of the rectangular bilayer upon detachment from the rectangular substrate. However, as the corners of the bilayer cannot be rolled simultaneously from both sides that are perpendicular to each other, we observed that the bilayer stopped rolling shortly after the rolling initiated. Therefore, any form of trigger, a use of tweezer in the current study for the thicker bilayers, is needed to break the symmetry of the equibiaxial stress level and thus to induce the bilayer to roll uniaxially along the direction that is set by the direction of applying the trigger. Using the tweezer method, we were able to form the uniaxially rolled structure for the thicker bilayers (Figure 2(a)). We observed that thinner bilayers (12 $\mu$m and 15 $\mu$m) spontaneously formed the uniaxially rolled structure upon detachment from the substrate without the need of the external trigger. We assume that even a small degree of anisotropy present inside the bilayer, for example, anisotropy of in-plane stress level generated during the spin-coating process or a difference in length of the side of the bilayer, is enough to induce the bilayer to roll uniaxially. In some cases, we observed the formation of cracks on the surface of the oxidized PDMS layer without the formation of the rolled structure (Figure 2(b)), which can be understood as the oxidized PDMS layer releases the tensile stress by being cracked.

Once the bilayer rolled due to the mismatch in the swelling ratios between the two layers, it maintains the uniaxially rolled cylindrical structure even after a complete evaporation of chloroform absorbed within the bilayer. We initially thought that the evaporation of chloroform from the bilayer should make each layer recover its lateral dimensions in the dry state that are identical to each other and thus the bilayer should unroll. However, we observed that the bilayer maintained its cylindrical structure without being unrolled even after the complete evaporation of the absorbed chloroform into the atmospheric air. We suppose that the maintenance of the rolled structure is primarily due to the adhesive energy between the two layers that exceeds or at least is comparable to the elastic deformation energy due to the rolling of the bilayer that has the identical lateral dimension for each layer.

Table 1: A list of the estimated and measured values used for the calculation of the elastic deformation energy for bending and the curvature of the rolled bilayer.

| | $t$ ($\mu$m) | $E$ (MPa) | $\nu$ | $\varepsilon$ |
|---|---|---|---|---|
| $PDMS_{un}$ | 12–67 | 3.5 [25, 26] | 0.5 | 0.15[A] |
| $PDMS_{ox}$ | 0.05 [24] | 500 [25, 26] | 0.5 | 0 |

[A] $\varepsilon$ of $PDMS_{un}$ is determined by measuring the length of the untreated PDMS film swollen by the chloroform vapor at the equilibrium state.

In the absence of covalent bonding at the interface of the two layers, the thermodynamic work of adhesion between the two layers ($W$) is expressed as $A(\gamma_{ox} + \gamma_{un} - \gamma_{ox\_un})$, where $\gamma_{ox}$ and $\gamma_{un}$ are the surface tensions of each layer, $A$ and $\gamma_{ox\_un}$ are the area of contact and the interfacial tension between the two layers, and ox and un denote the oxidized PDMS layer and the untreated PDMS layer, respectively. We used literature values of the two surface tensions, $\gamma_{ox}$ = 59 mN/m, which is roughly similar to that of glass (70 mN/m), and $\gamma_{un}$ = 22 mN/m [27] and crudely estimated the interfacial tension as the geometric mean of the two surface tensions; that is, $\gamma_{ox\_un}$ = 36 mN/m. In this case, the calculated work of adhesion per unit area of contact is 45 mN/m, which is within the range of the work of adhesion per unit area between the glass and the untreated PDMS that is reported in the previous literatures (12 mN/m–150 mN/m) [25, 28].

The elastic deformation energy for the rolling of the untreated PDMS layer can be calculated as

$$U_b = \frac{Dw}{2}\int_0^L \kappa^2 dx, \tag{1}$$

where $D = Et^3/12(1-\nu^2)$, $E$, $t$, $w$, $\nu$, $L$, and $\kappa$ are the bending rigidity, Young's modulus, the thickness, the width, Poisson's ratio, the distance along the circumferential direction ($x$), and the curvature of the untreated PDMS layer, respectively. Although Young's modulus of the oxidized PDMS layer is two orders of magnitude greater than that of the untreated PDMS layer [24, 26], the thickness of the former is three orders of magnitude smaller than that of the latter. Therefore, considering the relation of $D \sim Et^3$, we can effectively neglect the elastic deformation energy for the rolling of the oxidized PDMS layer. Table 1 summarizes the geometric and mechanical values used for the calculation, which are either measured in this study or estimated from the literatures. If we assume a constant curvature of the rolled bilayer, the density of the elastic deformation energy becomes

$$\frac{U_b}{wL} = \frac{U_b}{A} = \frac{D}{2R^2} = \frac{Et^3}{24\left(1-\nu^2\right)R^2}, \tag{2}$$

where $R$ is the radius of curvature of the rolled bilayer, which was measured using the optical microscope. The calculated value of $U_b/A$ for the PDMS bilayers with $t$ varying from 12 $\mu$m to 67 $\mu$m ranged from 10 mN/m to 103 mN/m, which is comparable to the calculated value of the work of adhesion per unit area $W/A$. Although the current

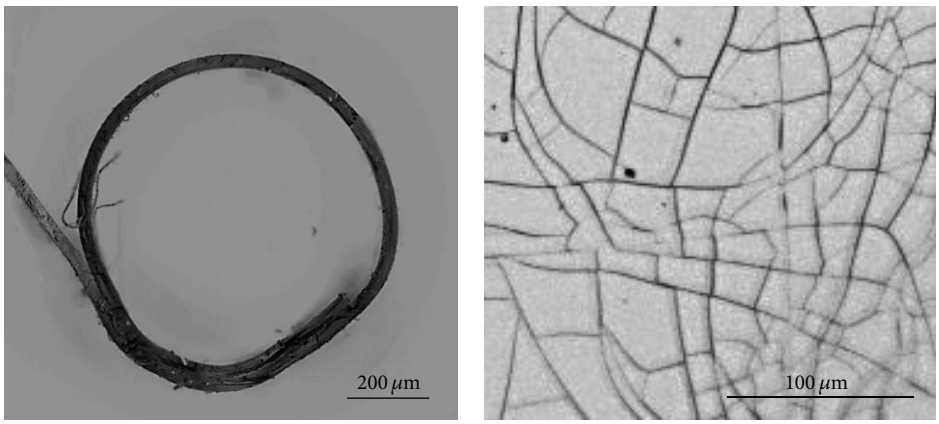


(a) (b)

Figure 2: (a) An optical micrograph of cross section of the rolled PDMS bilayer. (b) An optical micrograph of cracks generated on the surface of the oxidized PDMS layer.

comparison between the two energy densities is based on rough calculations with a number of estimated values, it is useful to infer why the rolled bilayer did not unroll even after the complete evaporation of the absorbed chloroform.

Next, we compared the measured radius of curvature of the rolled bilayer to the theoretical values calculated from Timoshenko's model. The model predicts the curvature of rolled (bent) bilayer that is composed of two linear elastic materials that expand in a different amount [22]. The radius of curvature of the rolled bilayer predicted by the model is

$$R = \frac{(t_{un} + t_{ox})\left[3(1+m)^2 + (1+mn)\left(m^2 + 1/mn\right)\right]}{6(\varepsilon_{un} - \varepsilon_{ox})(1+m)^2}, \quad (3)$$

where $m = t_{un}/t_{ox}$, $n = E_{un}/E_{ox}$, and $\varepsilon$ is the expansion of each layer. For the PDMS bilayer, $\varepsilon$ is defined as $l/l_0 - 1$, where $l$ and $l_0$ represent the length of each layer at the swollen state and the dry state, respectively. Figure 3 shows the plot of the curvature of rolled bilayer as a function of the bilayer thickness. Curvatures in the plot are either measured from the rolled bilayer fabricated in this study, estimated from Timoshenko's model using the variables in Table 1, or obtained from the previous literature where the experimental conditions used to fabricate the PDMS bilayer are almost identical except the bilayer thickness [4]. Although the bilayer thickness examined in this study extends over only an order of magnitude, the measured curvatures of rolled bilayer match reasonably well with the model.

Finally, we examined the feasibility of utilizing the rolled PDMS bilayer as the water impermeable microchannels. Figure 4 shows the centimeter-long microchannel formed by the rolled bilayer, which was connected to inlet and outlet tubing using small pieces of PDMS block attached on the glass substrate. Here, we examined whether the circumferential stress applied to the wall of the channel, that is, the rolled bilayer, due to the pressure of the aqueous solution flowing through the channel induces deformation or unrolling of the rolled bilayer. To visualize the flow in the channel, we perfused the channel with the aqueous solution containing

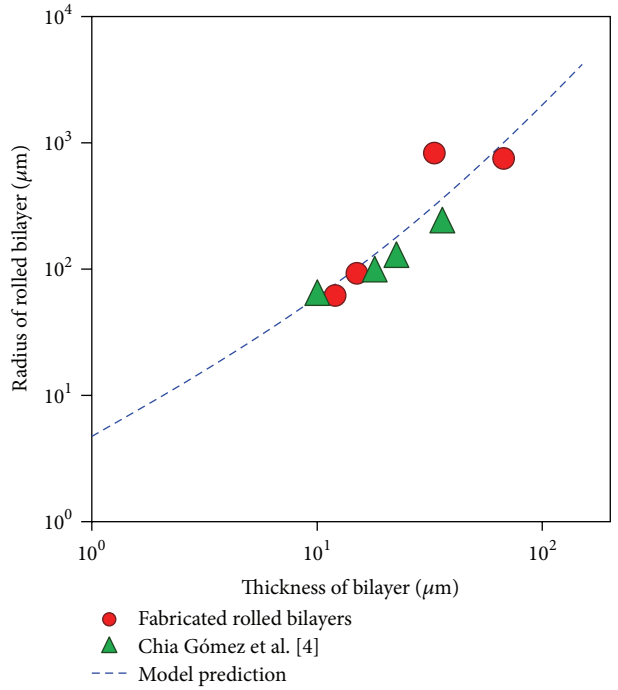


Figure 3: A plot of the radius of rolled bilayer as a function of the bilayer thickness. Radii in the plot are either measured from the rolled bilayer fabricated in this study (red circles), obtained from the previous literature (green triangles) [4], or predicted from Timoshenko's model (blue dashed line).

rhodamine B dye at a volumetric flow rate of roughly 1 mL/min using a syringe. If we assume the Hagen-Poiseuille flow, the pressure drop of the flow along the channel can be estimated as

$$\Delta p = \frac{128\,\mu L Q}{\pi d^4}, \quad (4)$$

where $\mu$, $L$, $Q$, and $d$ are the viscosity of the aqueous solution, the length of the channel, the volumetric flow rate, and the

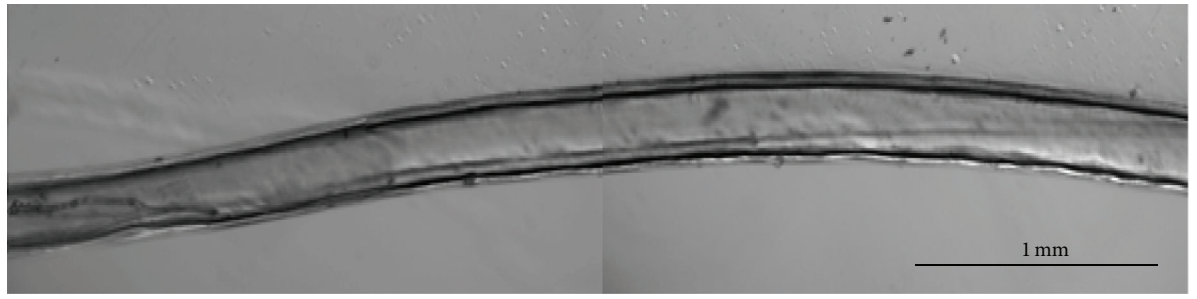


(a)

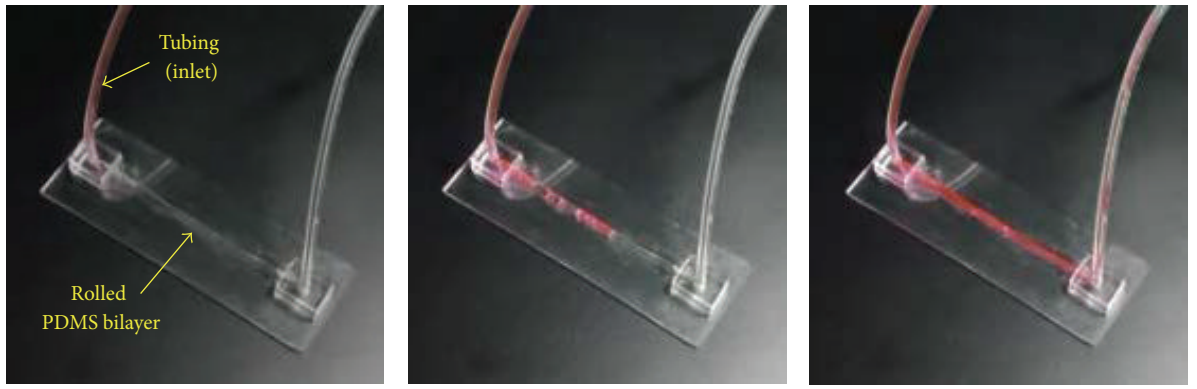


(b)

Figure 4: An optical micrograph of the centimeter-long rolled PDMS bilayer (a), which was connected to inlet and outlet tubing using small pieces of PDMS block to form a microchannel on the glass substrate (b). The aqueous solution containing rhodamine B dye was perfused into the microchannel at a volumetric flow rate of roughly 1 mL/min.

diameter of the channel, respectively, and we used roughly estimated values of 1 cP, 5 cm, 1 mL/min, and 0.5 mm for each variable. Here, we neglected the pressure drop by the flow within inlet and outlet tubing as $\Delta p \sim d^{-4}$ and $d_{\text{tubing}} \sim 2d_{\text{channel}}$ and also neglected the pressure drop by fittings. From (4), we can estimate the maximum internal gauge pressure of the fluid to be approximately 0.5 kPa at the inlet of the channel, which imposes the circumferential stress, or the hoop stress, of $\sigma_\theta = pR/t \sim 5$ kPa to the wall of the channel. As this value is much lower than Young's modulus of the channel, we can expect that the flow of the aqueous solution examined in this study induces negligible deformation, that is, stretching along the circumferential direction, of the channel. We also infer that the frictional force between the oxidized PDMS layer and the untreated PDMS layer is greater than or at least comparable to the hoop stress such that the bilayer does not unroll in the presence of the flow of the aqueous solution. As water is barely permeable to PDMS [23], the maximum normal stress acting on the wall of the channel is almost the same as the maximum pressure of the aqueous fluid within the channel, that is, 0.5 kPa. The friction coefficient of the contact between PDMS and Si substrate, which we assume to have the natural oxidized layer similar to the oxidized PDMS layer, is much greater than one at the normal stress around 0.5 kPa [12]. Therefore, we suppose that the resulting frictional force per a contact area provided sufficient resistance against the hoop stress, preventing unrolling of the rolled PDMS bilayer in the presence of the fluid flow. Experimentally, we observed neither appreciable deformation nor unrolling of the rolled bilayer.

## 4. Conclusions

In the current study, we induced uniaxial rolling of the PDMS bilayer composed of the oxidized PDMS layer and the untreated PDMS layer. Two layers differ from each other in the swelling ratio by the chloroform vapor, which resulted in the generation of in-plane equibiaxial stress within the bilayer. As the bilayers fabricated in this study are sufficiently thin, the primary mode of releasing the in-plane stress is to bend out-of-plane, which resulted in rolling of bilayer under equibiaxial stress from all four sides of the rectangular bilayer upon detachment from the substrate. Therefore, we gently pushed the bilayer from the one side using a tweezer to break the symmetry of the equibiaxial stress level in the bilayer and observed the formation of the uniaxial rolled PDMS bilayer. Once the bilayer rolled into the cylindrical structure, we compared the energy per unit area for adhesion and deformation by rolling and confirmed that the former is comparable in its magnitude to the latter. Therefore, we inferred that the bilayer maintained its rolled structure even in the dry state. In addition, we compared the microscopically measured curvature of the rolled bilayer to the theoretical

values calculated from Timoshenko's model and found that the model reasonably well predicted the experimental values. Finally, we predicted that the hoop stress, resulting from the pressure by the flow and acting on the wall of the channel made of the rolled bilayer, is small when compared to Young's modulus of the bilayer and the frictional force per a contact area between the two PDMS layers, which we supposed to be the reason why we observed neither appreciable deformation nor unrolling of the rolled bilayer by the flow of the aqueous solution. We expect that the mechanical aspects considered in this study can be similarly applied to explain the formation of rolled bilayers made of different materials, for example, metal, metal oxide, or composites, which have shown various applications in microfluidics, optical waveguides, and biomedical engineering.

## Conflict of Interests

The authors declare that there is no conflict of interests regarding the publication of this paper.

## Acknowledgments

This research was supported by Leading Foreign Research Institute Recruitment Program through the National Research Foundation of Korea (NRF) funded by the Ministry of Science, ICT & Future Planning (MSIP) (2013K1A4A3055268).

## References

[1] J. Yin, X. Han, Y. Cao, and C. Lu, "Surface wrinkling on polydimethylsiloxane microspheres via wet surface chemical oxidation," *Scientific Reports*, vol. 4, article 5710, 2014.

[2] P.-L. Ko, F.-L. Chang, C.-H. Li et al., "Dynamically programmable surface micro-wrinkles on PDMS-SMA composite," *Smart Materials and Structures*, vol. 23, no. 11, Article ID 115007, 2014.

[3] M. Guvendiren, S. Yang, and J. A. Burdick, "Swelling-induced surface patterns in hydrogels with gradient crosslinking density," *Advanced Functional Materials*, vol. 19, no. 19, pp. 3038–3045, 2009.

[4] L. P. Chia Gómez, P. Bollgruen, A. I. Egunov et al., "Vapour processed self-rolled poly(dimethylsiloxane) microcapillaries form microfluidic devices with engineered inner surface," *Lab on a Chip—Miniaturisation for Chemistry and Biology*, vol. 13, no. 19, pp. 3827–3831, 2013.

[5] E. P. Chan and A. J. Crosby, "Spontaneous formation of stable aligned wrinkling patterns," *Soft Matter*, vol. 2, no. 4, pp. 324–328, 2006.

[6] J. Hou, Q. Li, X. Han, and C. Lu, "Swelling/deswelling-induced reversible surface wrinkling on layer-by-layer multilayers," *The Journal of Physical Chemistry B*, vol. 118, no. 49, pp. 14502–14509, 2014.

[7] P. J. Flory and J. Rehner Jr., "Statistical mechanics of cross-linked polymer networks II. Swelling," *The Journal of Chemical Physics*, vol. 11, no. 11, pp. 521–526, 1943.

[8] E. Cerda, K. Ravi-Chandar, and L. Mahadevan, "Thin films: wrinkling of an elastic sheet under tension," *Nature*, vol. 419, no. 6907, pp. 579–580, 2002.

[9] E. Cerda and L. Mahadevan, "Geometry and physics of wrinkling," *Physical Review Letters*, vol. 90, no. 7, Article ID 074302, 2003.

[10] D. Huh, K. L. Mills, X. Zhu, M. A. Burns, M. D. Thouless, and S. Takayama, "Tuneable elastomeric nanochannels for nanofluidic manipulation," *Nature Materials*, vol. 6, no. 6, pp. 424–428, 2007.

[11] P. Kim, M. Abkarian, and H. A. Stone, "Hierarchical folding of elastic membranes under biaxial compressive stress," *Nature Materials*, vol. 10, no. 12, pp. 952–957, 2011.

[12] W. W. Tooley, S. Feghhi, S. J. Han, J. Wang, and N. J. Sniadecki, "Thermal fracture of oxidized polydimethylsiloxane during soft lithography of nanopost arrays," *Journal of Micromechanics and Microengineering*, vol. 21, no. 5, Article ID 054013, 2011.

[13] M. Christophersen, B. Shapiro, and E. Smela, "Characterization and modeling of PPy bilayer microactuators. Part 1. Curvature," *Sensors and Actuators, B: Chemical*, vol. 115, no. 2, pp. 596–609, 2006.

[14] Y. F. Mei, G. Huang, A. A. Solovev et al., "Versatile approach for integrative and functionalized tubes by strain engineering of nanomembranes on polymers," *Advanced Materials*, vol. 20, no. 21, pp. 4085–4090, 2008.

[15] G. Stoychev, N. Puretskiy, and L. Ionov, "Self-folding all-polymer thermoresponsive microcapsules," *Soft Matter*, vol. 7, no. 7, pp. 3277–3279, 2011.

[16] K. Kumar, B. Nandan, V. Luchnikov, E. B. Gowd, and M. Stammm, "Fabrication of metallic microtubes using self-rolled polymer tubes as templates," *Langmuir*, vol. 25, no. 13, pp. 7667–7674, 2009.

[17] C. Deneke and O. G. Schmidt, "Structural characterization and potential x-ray waveguiding of a small rolled-up nanotube with a large number of windings," *Applied Physics Letters*, vol. 89, no. 12, Article ID 123121, 2006.

[18] T. Kipp, H. Welsch, C. Strelow, C. Heyn, and D. Heitmann, "Optical modes in semiconductor microtube ring resonators," *Physical Review Letters*, vol. 96, no. 7, Article ID 077403, 2006.

[19] V. A. B. Quiñones, L. Ma, S. Li, M. Jorgensen, S. Kiravittaya, and O. G. Schmidt, "Localized optical resonances in low refractive index rolled-up microtube cavity for liquid-core optofluidic detection," *Applied Physics Letters*, vol. 101, no. 15, Article ID 151107, 2012.

[20] A. V. Prinz and V. Y. Prinz, "Application of semiconductor micro- and nanotubes in biology," *Surface Science*, vol. 532-535, pp. 911–915, 2003.

[21] V. Luchnikov, O. Sydorenko, and M. Stamm, "Self-rolled polymer and composite polymer/metal micro- and nanotubes with patterned inner walls," *Advanced Materials*, vol. 17, no. 9, pp. 1177–1182, 2005.

[22] S. Timoshenko, "Analysis of bi-metal thermostats," *Journal of the Optical Society of America*, vol. 11, no. 3, pp. 233–255, 1925.

[23] J. N. Lee, C. Park, and G. M. Whitesides, "Solvent compatibility of poly(dimethylsiloxane)-based microfluidic devices," *Analytical Chemistry*, vol. 75, no. 23, pp. 6544–6554, 2003.

[24] K. L. Mills, X. Zhu, S. Takayama, and M. D. Thouless, "The mechanical properties of a surface-modified layer on polydimethylsiloxane," *Journal of Materials Research*, vol. 23, no. 1, pp. 37–48, 2008.

[25] H. Kesari, *Mechanics of Hysteretic Adhesive Elastic Mechanical Contact between Rough Surfaces*, Stanford University, 2011.

[26] G. Bar, L. Delineau, A. Häfele, and M.-H. Whangbo, "Investigation of the stiffness change in, the indentation force and

the hydrophobic recovery of plasma-oxidized polydimethylsiloxane surfaces by tapping mode atomic force microscopy," *Polymer*, vol. 42, no. 8, pp. 3527–3632, 2001.

[27] M. K. Chaudhury and G. M. Whitesides, "Direct measurement of interfacial interactions between semispherical lenses and flat sheets of poly(dimethylsiloxane) and their chemical derivatives," *Langmuir*, vol. 7, no. 5, pp. 1013–1025, 1991.

[28] D. J. Quesnel, R. S. Rimai, and L. H. Sharpe, *Particle Adhesion: Applications and Advances*, CRC Press, New York, NY, USA, 2002.